Different emissive properties in dithiolate gold(I) complexes as a function of the presence of phenylene spacers†

Francesco M. Monzittu,[a] Vanesa Fernández-Moreira,[a] Vito Lippolis,[b] Massimiliano Arca,[b] Antonio Laguna[a] and M. Concepción Gimeno*[a]

A family of dinuclear neutral thiolate gold complexes of the type $RPh_2PAuS(C_6H_4)_nSAuPPh_2R$ (n = 2, 3), $RPh_2PAuS(C_6H_4)S(C_6H_4)SAuPPh_2R$, $RPh_2PAuSCH_2(C_6H_4)_2CH_2SAuPPh_2R$ where R represents a pyridine or a phenyl ring, have been prepared and fully characterized. X-ray crystallographic studies showed the presence of aurophilic interactions for those species bearing two phenylene spacers between the gold metal centres, leading to infinite chains. The complexes are emissive in the solid state. Theoretical calculation together with the photophysical analysis seems to indicate that the main excitations involved in the emissive processes are due to a mixture of ILCT transition involving the thiolate and the conjugated phenylene rings and LL'CT transitions comprising the thiolate and the pyridine or phenyl from the phosphine fragment which contrast with the typical gold thiolate emission, LMCT from the thiolate fragment to the metal center.

Introduction

Phosphine-gold(I)-thiolate derivatives have been intensely studied due to their potential applications in the development of new materials,[1] chemosensors[2] as well as in the medical field as novel therapeutic agents.[3] These wide range of possibilities have awakened an increasing interest in studying their structure and photophysical properties. In particular, thiolate derivatives are versatile ligands that allow the synthesis of coordination compounds with different features. They can accommodate one, two and even three gold centers,[4] which might promote a completely different spatial distribution. Such great diversity of possible structures could induce diverse photophysical properties, either because gold(I)-gold(I) interactions can occur, or simply because the different packaging modes would alter the luminescence. Typically emission of thiolate-Au phosphine derivatives takes place between 400 nm and 700 nm and it is mainly originated from ligand to metal charge transfer (LMCT) transitions, from the thiolate fragment to the gold metal center. However, thiolate to phosphine charge transfer (LL'CT), gold to thiolate charge transfer (MLCT) and thiolate centered (LC) transitions have been also described in the literature for these type of species.[5] In addition, the incorporation of phenyl spacers between the metals centers seemed to confer a different approach to the conventional photophysical properties of gold-thiolate derivatives. Previous work performed by Kosehovoy and coworkers described that, in those cases, thiolates and phosphine intraligand charge transfer processes are the primary responsible transition for the emission.[6] Furthermore, aurophilic interactions are relegated to a secondary role as their presence or absence is irrelevant. More examples that support this theory were also reported for dinuclear gold complexes with diphosphanes containing alkyne and/or phenylene spacers. Once again, the presence of phenylene spacers in the backbone seems to control the photophysical properties of the complexes. Therefore, in this work, a family of dithiolate phenyl derivatives was chosen as spacers to synthesize a new series of bimetallic thiolate-gold(I) phosphine derivatives. Then, a thorough analysis of their crystalline structure, together with photophysical studies and theoretical calculations will attempt to shed a bit of light on the influence of phenylene spacers in the emission properties of thiolate-gold(I) phosphine derivatives.

Synthesis and characterisation

Dithiolate Au^I Complexes

Gold(I) complexes (**1** - **8**) were synthesized by reaction of the corresponding di-thiolate ligand with either $ClAuPPh_3$ or $ClAuPPh_2Py$ in presence of cesium carbonate to assist the thiol deprotonation and subsequent metal coordination (see Scheme 1). Spectroscopic characterization of each gold complex was performed using IR, ^1H, ^{31}P and ^{13}C NMR spectroscopy, and UV−vis spectroscopic measurements. Infrared spectroscopy showed in all cases the disappearance of ν(S-H) stretching band at *ca.* 2550 cm^{-1} indicating the deprotonation of the thiol functions. ^{31}P-NMR spectra presented a significant low-field shift of the phosphine peak, from *ca.* 33 ppm to *ca.* 38 ppm after coordination of the dithiolate species to the gold phosphine derivatives, which is in agreement with analogous NMR spectroscopy data reported for different thiolate-gold(I) phosphine complexes.[7] Moreover, the chemical shifts observed in ^{13}C-NMR and ^1H-NMR spectroscopy corroborates the success of the coordination reaction. Thus, the synthesized complexes **1-8** showed, in all cases, that the SC_{ipso} carbons were shifted to low field as well as the disappearance of the signal belonging to S-H protons in ^1H-NMR spectroscopy. Further analytical data provided by mass spectrometry is in concordance with the expected gold(I) species **1** – **8** (Table 1). Additionally, suitable crystals of **2**, **4**, **5** and **6** were obtained that allowed structural characterization by X-ray diffraction.

Scheme 1. Synthesis and numbering of gold(I) species synthesised. (i) Cs_2CO_3, DCM / MeOH, 2h, Ar.

Table 1. Relevant spectroscopic data for complexes **1-8**

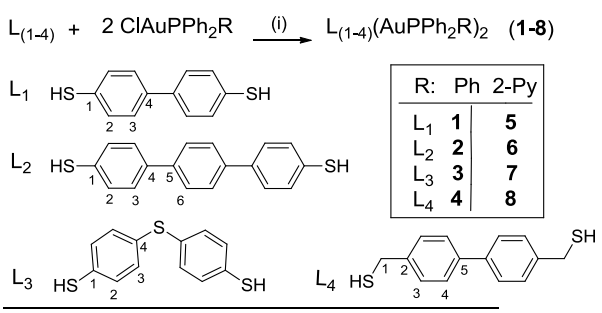

Complex	$^{31}P\{^1H\}$ (ppm)	$^{13}C\{^1H\}$ (ppm)[a]	*m/z*
1	38.75	141.7	1135.0[b]
2	38.77	142.8	1210.1[c]
3	38.88	142.3	1166.0[c]
4	37.85	147.6	1162.1[c]
5	37.98	141.2	1137.1[c]
6	37.13	142.2	1213.2[b]
7	38.01	142.6	1168.9[c]
8	35.97	146.7	1164.9[c]

NMR spectra measured in CD_2Cl_2. [a]-SC_{ipso}. [b]MS(ES). [c]MS(MALDI+).

X-ray analysis

Single crystals suitable for X-ray diffraction analysis of complexes **2**, **4**, **5** and **6** were obtained by slow diffusion of hexane into a dichloromethane solution. The unit cells of complexes **2**, **4**, and **5** are formed by 4 complex molecules each, whereas only 2 complex molecules are displayed in the unit cell of complex **6**. Moreover, all of them presented half molecule as asymmetric unit and species **2**, **4** and **6** displayed an inversion center. As expected, in all cases the gold atom presented a distorted linear geometry with a S-Au-P angles between 175.06(4)° and 179.16(7)° and the Au-S and Au-P distances ranging from 2.286(2) Å to 2.3048(11) Å and from 2.244(2) Å to 2.2597(11) Å, respectively, which are within the normal values for S-Au-P derivatives.[8,7c] A summary of distances and angles is presented in Figure 1.

Only complex **5** showed intermolecular $Au^I\cdots Au^I$ interaction of 3.0336(11) Å, which lead to the formation of infinite chains in the crystal lattice together with point to face, C-H$\cdots\pi$, interactions[9] between the phenylene spacer and one adjacent PPh_2Py unit and between two adjacent PPh_2Py molecules, see Fig. 2. Point to face interactions between the phenylene spacers and the phosphine derivative units were also observed for complexes **2** and **6**. Furthermore, these species presented S-S and S-(H-$PyPh_2P$) short contacts at *ca*. 3.235 Å and 2.743 Å, respectively. These short contacts and the C-H$\cdots\pi$ interactions are responsible for their molecular packing (see ESI†, Figs. S1-S3). The closest $Au^I\cdots Au^I$ distances for complex **2** and **6** are 4.565 Å and 5.484 Å respectively, values relatively long to be considered aurophilic interactions (3.0 - 3.3 Å).[10]

In contrast, complex **4** did not show any phenylene-PPh_3 interaction and presented a torsion angle between the phenylene spacers of 1.1(4)°. Such torsion angle is relatively shorter than those founded for complexes **2**, **5** and **6**, values between 30.63(8)° and 35.31(1)° (see Fig. 1).The short contacts present in complex **4** are those formed between the gold atom and a proton from a neighboring triphenylphosphine unit, the distance $Au^{I}\cdots H$ is 2.850 Å ESI†, Fig. S4).

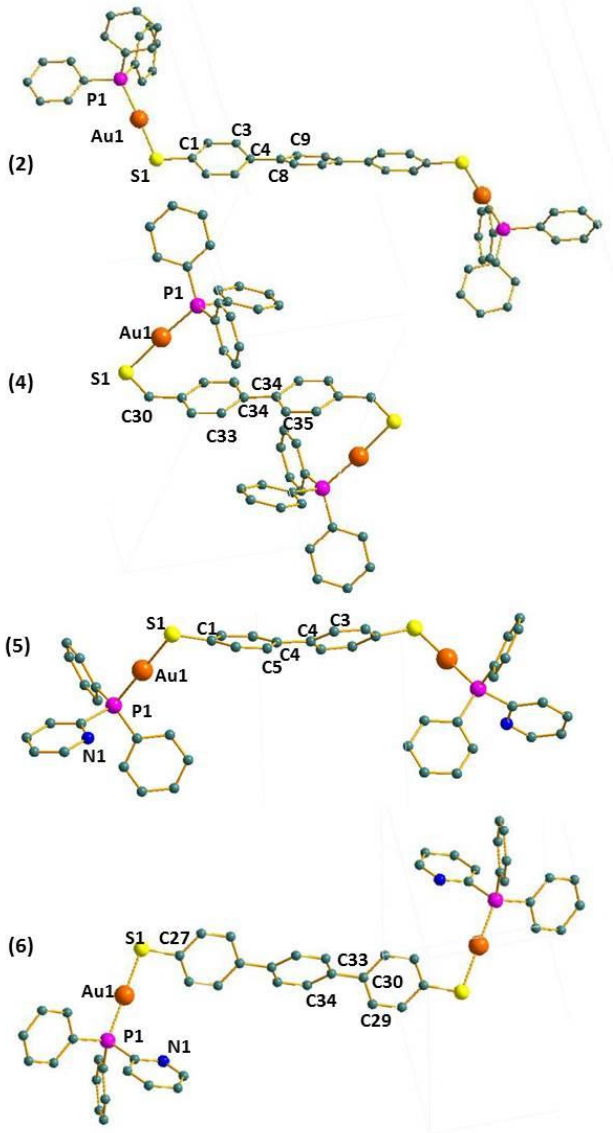

Figure 1. Diamond diagrams of species **2**, **4**, **5**, **6** (Protons omitted for clarity). Selected bond length, angles and torsion angles for: (**2**) Au(1)-S(1) 2.3048(11) Å, Au(1)-P(1) 2.2597(11) Å; S(1)-Au(1)-P(1) 175.06(4) °, Au(1)-S(1)-C(1) 109.34(16) °; C(9)-C(8)-C(4)-C(3) 30.63(8) °; (**4**) Au(1)-P(1) 2.2582(6) Å, Au(1)-S(1) 2.3035(6) Å; P(1)-Au(1)-S(1) 176.13(2)°, C(30)-S(1)-Au(1) 101.99(8)°; C(33)-C(34)-C(34)-C(35) 1.1(4)° (**5**) Au(1)-S(1) 2.286(2) Å, Au(1)-P(1) 2.244(2) Å, Au(1)-Au(1) 3.0336(11) Å, S(1-)Au(1)-P(1) 179.16(7)°, S(1)-Au(1)-Au(1) 76.83(5)°, P(1)-Au(1)-Au(1) 10.99(7)°, C(1)-S(1)-Au(1) 104.4(2)°; C(3)-C(4)-C(4)-C(5) 30.97(1)°; (**6**) Au(1)-P(1) 2.257(2) Å, Au(1)-S(1) 2.296(2) Å, P(1)-Au(1)-S(1) 178.16(9)°, Au(1)-S(1)-C(27) 104.1(3)°, C(29) C(30)-C(33) C(34) 33.77(1)°.

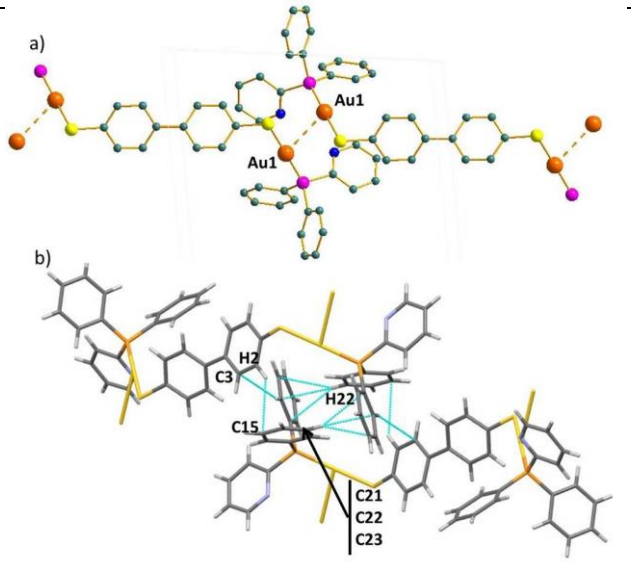

Figure 2. (a) Diamond diagrams of aurophilic interactions and (b) Ortep diagram of C-H···π interactions in complex **5**. Au(1)···Au(1): 3.0336(11)Å, C(15)-H(2)···π: 2.894 Å, C(3)-H(22)···π: 2.734 Å, C(21)-H(13)···π: 2.792 Å, C(22)-H(13)···π: 2.734 Å, C(23)-H(13)···π: 2.866 Å.

Optical properties

As commented previously **L1** and **L2** are similar ligands where the donating groups, the thiolates, are connected by 2 and 3 phenyl rings, respectively, acting as spacers, thus allowing the electronic communication between the two ends of the ligand. However, **L3** and **L4** do not have such property due to the presence of a thio-ether between the two phenyl rings in the case of **L3**, and a methylene group between the phenyls and the donating thiolates in **L4**. As a result of this, a remarkable difference in the optical properties is prone to be observed for the 4 families of complexes. UV-visible spectra of ligands **L1**–**L4** and complexes **1**–**8** were performed in solid state. Ligands **L1**, **L2**, and **L3** showed the same absorption profile, a single unstructured band around 300 nm that could be assigned to $\pi \rightarrow \pi^*$ transitions within the phenylene rings. By contrast **L4** displayed two absorption bands centered at 215 nm and at 277 nm. In this case, the high energetic band transition could be assigned to $n \rightarrow \sigma^*$ transitions within the S-C bonds (-CH_2S-fragment), whereas the peak at 277 nm might be due, once again, to $\pi \rightarrow \pi^*$ transitions in the phenylene rings.[11] Analysis of the complexes absorption profile showed also a similar pattern to that of the single ligands. The maxima absorption is generally red-shifted of about 30 nm upon complexation which could be tentatively assigned to transitions involving the thiolate and the conjugated phenylene rings as well as the thiolate and the pyridyl or phenyl groups from the phosphine fragments, *i.e.* LL'CT and ILCT respectively, see Fig. 3 for complexes **1** and **5** (see ESI†, Fig. S5 for other ligands and Fig. S6 for the complexes). These results contrast with the typical behaviour observed for gold(I) thiolate complexes, *i.e.* electronic transitions from the thiolate to the gold metal center, LMCT,[5b,12] highlighting the important role of the phenylene spacers in the spectroscopic properties of these family of complexes.

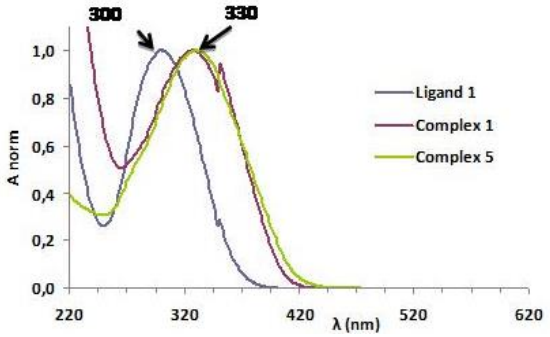

Figure 3. DRUV spectra of **L1** and complexes **1** and **5**.

Emission and excitation spectra of ligands **L1**-**L4** and complexes **1**-**8** were collected in solid state at 298 K and 77 K. These experiments were performed only in solid state due to the low solubility of the complexes. Table 2 includes the excitation and emission data and Figure 4 shows some examples of the emission spectra of these complexes (see ESI†, Fig. S7, for the emission spectra of complexes **2**, **4**, **5**, **7** and ligand **L2**).

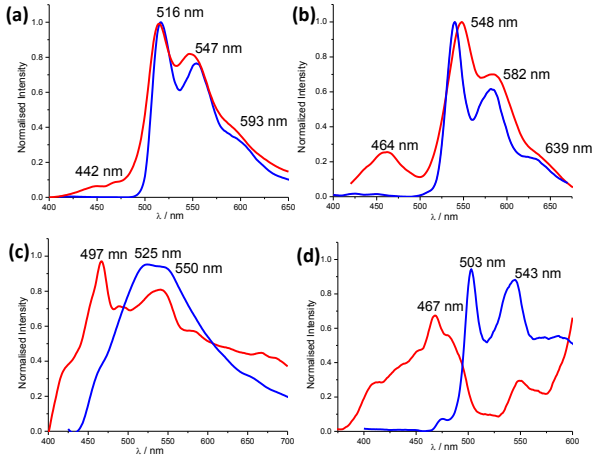

Figure 4. Emission spectra at 298 K (red line) and 77 K (blue line) of species (a) **1**, (b) **6**, (c) **3**, (d) **8** (metallic species derived from **L1**, **L2**, **L3** and **L4** respectively).

In all cases, **L1**, **L3** and **L4** showed a weak luminescence; only **L2** displayed a structured emission band centered at c.a. 400 nm that could be assigned to intra-ligand charge transfer (ILCT) transitions within the phenylene rings. Luminescence of $Au(PPh_3)Cl$ and $Au(PPh_2Py)Cl$, gold complexes used as the starting material in the reactions, comes from transitions within the phosphine unit.[13] Analysis of the photophysical properties of complexes **1**-**8** suggests that the different emission and excitation spectra patterns seem to be more influenced by the different ligands structure than by the metallic fragment, *i.e.* –$(AuPPh_3)$ and –$(AuPPh_2Py)$. Specifically, complexes **1**, **2**, **5** and **6**, metallic species formed with **L1** and **L2,** have a similar behavior. At room temperature they present two emission bands at *ca.* 450 nm and 550 nm, being the latter a well resolved structured band as well as the main component of emission. However, at 77K the emission centered at *ca.* 450 nm disappears and only the well-structured band at *ca.* 550 nm remains, which did not show any apparent change. The energy gap between vibronic peaks, between 1200 and 1300 cm^{-1}, is typical for the excited states of aromatic systems, emphasizing the importance of the conjugated phenylene rings of the ligands **L1** and **L2** in the excited state. Therefore, it seems reasonable to associate the highly structured band to intra-ligand charge transfer (ILCT) transitions, involving the thiolate and the conjugated phenylene rings. Moreover, ligand to ligand charge transfer (LL'CT) transitions are also prone to happen from the thiolate to the pyridyl or phenyl groups from the phosphine fragments. In fact, complex **5** is thought to have both types of transitions as the emission profile is not as well structurally defined as the one seen for **1**, **2** and **6** which might indicate an energy transfer process from the thiolate to the pyridyl of the phosphine fragment, in concordance with previous reports on similar complexes.[6,14] Moreover, lifetimes in the microsecond domain together with the considerable large Stoke shift suggest a phosphorescent nature of this emission. It is also worth noting the larger lifetime value of complex **2** (662 μs) in comparison with that of complex **1** (54 μs). Such difference was also previously seen in similar species and it could be related to the increase in the number of phenylene spacers, *i.e.* from 2 in complex **1** to 3 in complex **2**.[6] On the contrary, the band at c.a. 460 nm which is only observed at 298 K could be assigned LC (-PPh_3 /-PPh_2Py) emission.[15, 16] At the same time, the short lifetime observed for this transition might indicate a fluorescent transition character. As commented previously, photophysical behavior of complexes **3**, **7**, **4** and **8,** metallic species derived from **L3** and **L4** respectively**,** is likely to differ from those observed for complexes **1**, **5**, **2** and **6** due to the different electronic communication within the ligand system. Therefore, complexes **3** and **7**, showed a broad band at 467 nm and a shoulder at ca. 525 nm of similar intensity whereas complexes **4** and **8** presented a peak 467 nm and a much smaller band around 550 nm at room temperature. These emissions are relatively weak in comparison with those seem for complexes **1**, **2**, **5** and **6** in the same conditions and they are not observable with the naked eye under irradiation with a handed UV-lamp. In both cases, the band at c.a. 460 nm could be thought to be a LC (-PPh_3/PPh_2Py) transition.[15, 16] On the contrary, at 77 K these complexes showed an increase in the luminescence intensity as well as changes in the band profile. A featureless broad emission band at *ca.* 540 nm and two differentiated bands at c.a. 503 nm and 543 nm remained for complexes **3** and **7** and complexes **4** and **8** respectively. Assignation of those bands seems to have a much more complicated explanation, where not only the phenyl rings and the thiolate could be implicated but also, the ancilliary ligands, i.e. PPh_3 and PPh_2Py, and the thioether in the case of complexes **3** and **7**. Typically the emission displayed by luminescent phosphane-gold(I)-thiolate fragments is attributed to ligand-to-metal charge transfers (LMCT), which could be modified by changes in both the phosphine and the thiolate ligand and also by the presence of $Au^I \cdots Au^I$ interactions.[5b] However, in this case, ancillary ligands, the thiolates and the phenylene spacers appear to be the primary contributors to the luminescence of these complexes and aurophilic interactions do not seem to influence the photophysical behavior. Such results suggest that the phenylene spacers play a key role in the photophysical properties. Recently, a similar behavior was observed for gold(I)-thiolate complexes with phosphines bearing phenylene spacers.[6]

Table 2. Luminescence data for complexes **1**-**8**.

	λ_{em} / nm (τ / μs) 298 K	λ_{em} / nm 77 K
1	442 (12), 516, 547$_{sh}$, 593$_{sh}$ (54) [a]	516, 554$_{sh}$, 598$_{sh}$ [a]
2	448 (10), 544, 585 $_{sh}$, 632$_{sh}$ (662) [b]	540, 580$_{sh}$, 630$_{sh}$ [c]
3	467 (12), 546 (12) [a]	532 [d]
4	467 (12)[e]	473, 502, 541$_{sh}$ [f]
5	418, 467, 513, 552$_{sh}$ [c]	510, 550$_{sh}$, 590$_{sh}$ [g]
6	464, 548, 582$_{sh}$, 639$_{sh}$ [d]	539, 582$_{sh}$, 632$_{sh}$ [c]
7	467, 546[h]	532[g]
8	466	473, 503, 542$_{sh}$ [f]

[a] λ_{exc} = 380 nm, [b] λ_{exc} = 385 nm, [c] λ_{exc} = 370 nm, [d] λ_{exc} = 400 nm, [e] λ_{exc} = 325 nm [f] λ_{exc} = 350 nm, [g] λ_{exc} = 390 nm, [h] λ_{exc} = 360 nm.

DFT calculations

In order to investigate the origin of the electronic transitions responsible for the absorption and emission properties of complexes **1**-**8**, DFT calculations were carried out on representative members of the complex families. In particular, the investigation concerned complex **4** and a discrete model of complex **5**, **5'**, featuring two L_1'AuPPh$_2$Py units joined by Au···Au interactions (L_1' = monothiolate form of L_1) (see the Experimental Section for the computational set-up chosen). Ground State geometry optimization was performed in both cases and a good agreement was found between calculated and experimental geometrical parameters. In particular, for complex **4** the calculated Au-P (2.313 Å) and Au-S (2.327 Å) bond distances are slightly longer than the structural values, with a calculated S-Au-P angle of 178.64°, and the aromatic rings of the phenylene spacer being coplanar as observed in the crystal structure. Also the optimized geometry of complex **5'** very well reproduces the structural features of the repetitive unit in the 1D chains held by Au···Au interactions in complex **5**. The calculated Au-P, Au-S and Au···Au distances (2.347, 2.316, and 3.303 Å, respectively) are slightly overestimated. The gold-gold distance, although overestimated, accounts for a direct metal-metal interaction, also testified by a non-negligible Wiberg bond index (0.150). The calculated bond angles are very close to those observed experimentally (P-Au-S 177.52, P-Au-Au 104.15, S-Au-Au 77.97°), including the torsion angle between the aromatic rings of the dithiolate spacer (34.74°).

The pattern of singlet excited states (ESs) was computed at the TD-DFT level for **4** and **5**' at their optimized geometries. In both cases a good agreement was found between the experimental DRUV spectra recorded for **4** and **5** and the spectra simulated on the basis of computed vertical absorption spectra (see Fig. 3 for **5'** and Fig. S8 in the ESI† for **4**). In particular, the experimental broad absorption band observed at 320 nm for **5** is computed for **5'** to be the sum of different electronic transitions, the most intense falling at 396, 321 and 249 nm and arising from the vertical transitions $S_0 \rightarrow S_1$, $S_0 \rightarrow S_{16}$ and $S_0 \rightarrow S_{55}$, respectively (1, 2, and 3 in Figs. 5 and 6). The transition $S_0 \rightarrow S_1$ (calculated at E = 3.130 eV, oscillator strength f = 0.131) presents a contribution from the 254/HOMO→255/LUMO and 253/HOMO-1→256/LUMO+1 monoelectronic excitations from molecular orbitals (MOs) mainly localized on the S atom to orbitals mainly localized on the pyridine ring and therefore of the type LL'CT (Fig. 6). The transition $S_0 \rightarrow S_{16}$ (the most intense, f = 0.356; E = 3.867 eV) arises mainly from four excitations from 254/HOMO or 253/HOMO-1 MOs to MOs mainly localized on the pyridine ring (264/LUMO+9 and 262/LUMO+7) or on the aromatic rings of the phenylene spacer (263/LUMO+8), so that these transitions can be considered LL'CT and ILCT in nature.

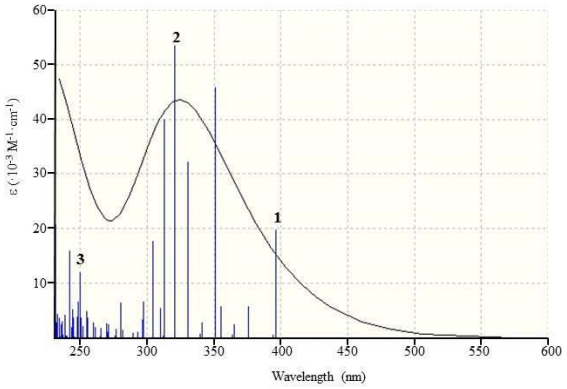

Figure 5. Simulated absorption spectrum for **5'** in the gas phase with calculated TD-DFT singlet vertical transitions.

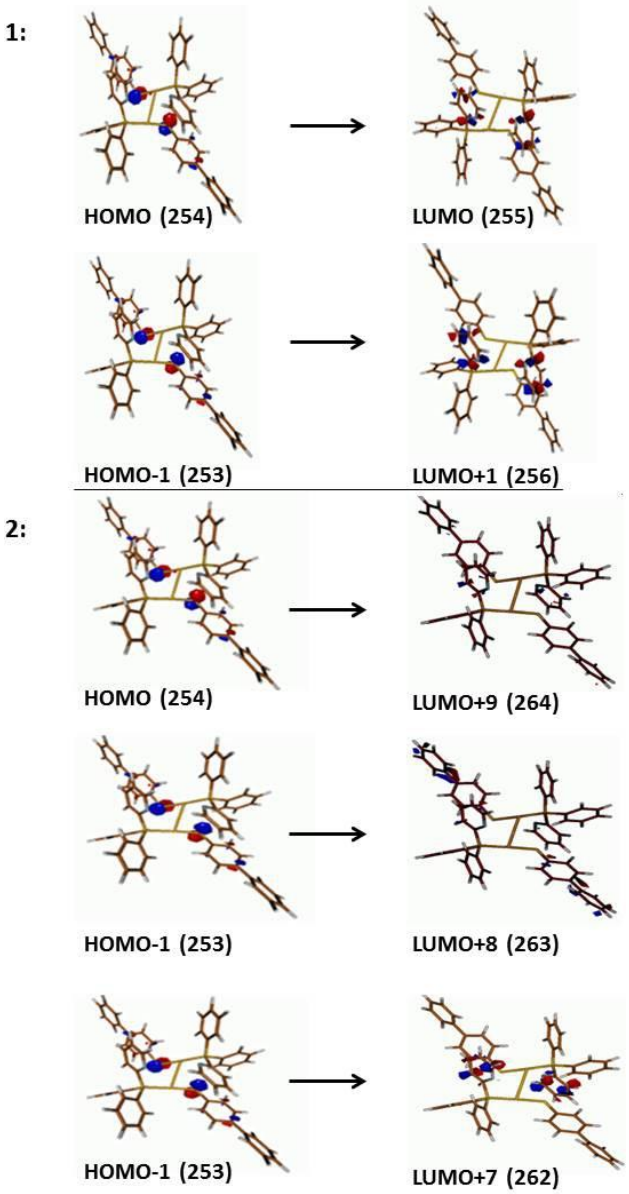

Figure 6. Isosurface drawings of the Kohn-Sham MOs calculated for **5'** involved in the principal singlet vertical electronic transitions (1 and 2 in Fig. 5). Contour value = 0.05 e.

Transitions involving the Au^I centres fall in the UV region such as the $S_0 \rightarrow S_{55}$ calculated at 250 nm (E = 4.960 eV; f = 0.079). These MLCT transitions involve the excitations from MOs localized on the Au and S atoms to those on the ligand and the pyridine rings in particular. No transitions are found which involve a charge transfer between the two interacting Au^I centres.

Analogous conclusions can be drawn by analysing the simulated spectrum of **4**. The most intense computed vertical transitions correspond to mono-electronic excitations of the type LL'CT and ILCT. Excitations involving the metal centres are calculated at higher energies and are of the type MLCT (see ESI†, Fig. S9).

Conclusions

In summary, we have synthesised and characterised new dithiolate gold phosphine complexes with different spacers between both thiolate units. Structural characterization by X-ray diffraction studies showed that only in one case, complex **5**, aurophilic interactions are present and led to the formation of a chain polymer. Theoretical calculations combined with photophysical analysis indicate that the main emission origins from excited states due to a mixture of ILCT transition involving the thiolate and the conjugated phenylene rings and LL'CT transitions comprising the thiolate and the pyridine or phenyl from the phosphine fragment. Radiative relaxation could also occur through intersystem crossing (ISC) from these singlet excited states to triplet states. These results emphasize the importance of the phenylene spacers between the metals centers in the luminescent properties, as the typical gold thiolate emission was normally assigned to LMCT from the thiolate fragment to the metal center.

Experimental Section

Instrumentation

Mass spectra were recorded on a BRUKER ESQUIRE 3000 PLUS, with the electrospray (ESI) technique and on a BRUKER MICROFLEX (MALDI-TOF), with a Ditranol or a T-2-(3-(4-tButyl-phenyl)-2-methyl-2-propenylidene)malononitrile matrix. ^1H, $^{13}C\{H\}$ and ^{31}P NMR spectroscopy, including 2D experiments, were recorded at room temperature on a BRUKER AVANCE 400 spectrometer (^1H, 400 MHz, ^{13}C, 100.6 MHz, ^{31}P, 162 MHz) with chemical shifts (δ, ppm) reported relative to the solvent peaks of the deuterated solvent. Infrared spectra were recorded in the range 400-250 cm^{-1} on a Perkin-Elmer Spectrum 100 FTIR spectrometer. UV/vis spectra were recorded with Jasco V-670 spectrophotometer fitted with a Praying Mantis diffuse reflectance accessory. Room temperature steady-state emision and excitation spectra were recorded with a Jobin-Yvon-Horiba fluorolog FL3-11 spectrometer fitted with a JY TBX picosecond detection module. Phosphorescence lifetimes were recorded with a Fluoromax phosphorimeter accessory containing a UV xenon flash tube.The lifetime data were fit using Origin 5.0.

Starting materials

$ClAuPPh_3$, $ClAuPPh_2Py$ were prepared according to literature procedures.[17] Other starting materials and solvents were purchased from commercial suppliers and used as received unless otherwise stated.

General procedure for the synthesis of the complexes 1-8

Synthesis of 1: Cs_2CO_3 (53.8 mg, 0.246 mmol) was added to a solution of **L1** (22.5 mg, 0.103 mmol) in 15 ml of methanol. After stirring for few minutes a solution of $ClAuPPh_3$ (102.3 mg (0.206 mmol) in 2 ml of DCM was added dropwise the mixture and it was further stirred for one hour at room temperature until a solid appeared. The precipitate was separated by filtration and washed several times with methanol and diethyl ether to give **1** as a pale green solid (85.3 mg, 73%). NMR (CD_2Cl_2 20°C): ^{31}P NMR (162 MHz) 38.75, s; ^1H NMR (400 MHz) 7.27 – 7.33, m, 4H (3-Thiol), 7.46 – 7.64, m, 34H (Ph and 2-Thiol); ^{13}C NMR (101 MHz) 126.7, s, (2-Thiol), 130.0, d (*J* = 11.4 Hz), (*m*-Ph), 130.6, s, (ipso-Ph), 132.5, d, (*J* = 2.5 Hz), (*p*-Ph), 132.3, s, (1-Thiol), 135.0, d, (*J* = 13.8 Hz), (*o*-Ph), 136.6, s, (4- Thiol), 141.7, s, (3-Thiol).). Anal. Calcd for $C_{48}H_{38}Au_2P_2S_2$: C, 50.80; H, 3.38; Found: C, 50.47; H, 3.15; MS (ES): m/z calcd for $C_{48}H_{38}P_2S_2Au_2$ (M^+) 1134.1, found 1135.0.

Synthesis of 2: This compound was prepared similarly to **1** using **L2** instead of **L1**. The product was obtained as a yellow solid (90.0 mg, 81 % yield).

NMR (CD_2Cl_2 20°C): ^{31}P NMR (162 MHz) 38.77, s; ^1H NMR (400 MHz) 7.37 – 7.41, m, 4H (6-Thiol), 7.47 – 7.64, m, 38H (Ph, 3-Thiol and 2- Thiol); ^{13}C NMR (101 MHz) 127.1, s, (3-Thiol), 127.5, s, (2-Thiol), 130.1, d (*J* = 11.5 Hz), (*m*-Ph), 130.7, s, (ipso-Ph), 132.5, d (*J* = 2.5 Hz), (*p*-Ph), 133.5, s, (6-Thiol), 135.0, d (*J* = 13.8 Hz), (*o*-Ph), 136.3, s, (5-Thiol), 140.0, s, (4-Thiol), 142.8, s, (1-Thiol). Anal. Calcd for $C_{54}H_{42}Au_2P_2S_2$: C, 52.78; H, 3.61; Found: C, 52.93; H, 3.23; MS(MALDI+/DIT): *m/e* = 1210.1 $[M]^+$.

Synthesis of 3: This compound was prepared similarly to **1** using **L3** instead of **L1**. The product was obtained as a yellow solid (97.5 mg, 83 % yield).

NMR (CD_2Cl_2 20°C): ^{31}P NMR (162 MHz) 38.88, s; ^1H NMR (400 MHz) 7.01 – 7.06, m, 4H (3-Thiol), 7.42 – 7.60, m, 34H (Ph and 2-Thiol); ^{13}C NMR (101 MHz) 129.6, d (*J* = 11.5 Hz), (*m*-Ph), 130.1, s, (ipso-Ph), 130.8, s, (4-Thiol), 131.2, s, (3-Thiol), 132.1, d (*J* = 2.5 Hz), (*p*-Ph), 133.2, s, (2-Thiol), 134.6, d (*J* = 13.8 Hz), (*o*-Ph), 142.3, 2, (1-Thiol). Anal. Calcd for $C_{48}H_{48}Au_2P_2S_3{\cdot}0.5CH_2Cl_2$: C, 48.17; H, 3.25; Found: C, 47.97; H, 2.95; MS(MALDI+/DCTB): *m/e* = 1166.0 $[M]^+$.

Synthesis of 4: This compound was prepared similarly to **1** using **L4** instead of **L1**. The product was obtained as a white solid (74.4 mg, 74 % yield).

NMR (CD_2Cl_2 20°C): ^{31}P NMR (162 MHz) 37.85, s; ^1H NMR (400 MHz) 4.16, s, 4H (1-Thiol), 7.28 – 7.33, m, 4H (4-Thiol), 7.37 – 7.51, m, (Ph and 3-Thiol); ^{13}C NMR (101 MHz) 32.9, s, (1-Thiol), 127.4, s, (4-Thiol), 129.6, s, (3-Thiol), 129.8, d (*J* = 11.2 Hz), (*m*-Ph), 130.9, d (*J* = 53.7), (ipso-Ph), 132.2, d (*J* = 2.4 Hz), (*p*-Ph), 134.9, d (*J* = 14.0 Hz), (*o*-Ph), 139.1, s, (5-Thiol), 147.6, s, (2-Thiol). Anal. Calcd for $C_{50}H_{42}Au_2P_2S_2$: C, 51.62; H, 3.64; Found: C, 51.37; H, 3.46; MS(MALDI+/DCTB): *m/e* = 1162.1 $[M]^+$.

Synthesis of 5: This compound was prepared similarly to **1** using $ClAuPPh_2Py$ instead of $ClAuPPh_3$. The product was obtained as a pale green solid (82.5 mg, 79%)

NMR (CD_2Cl_2, 20°C): ^{31}P NMR (162 MHz) δ 37.98, s; ^1H NMR (400 MHz) 7.27 -7.34, m, 4H (3-Thiol), 7.38 - 7.45, m, 2H (5-Py), 7.45 - 7.60, m, 16H (Ph and 2-Thiol), 7.68 - 7.77, m, 8H (Ph), 7.82, ddd (*J* = 7.7, 3.8, 1.8 Hz), 2H (4-Py), 7.89, t (*J* = 7.4 Hz), 2H (3-Py), 8.77 - 8.83, m, 2H (6-Py); ^{13}C NMR (101 MHz) 125.6, d (*J* = 2.4 Hz), (5-Py), 126.4, s (3-Thiol), 129.5, d (*J* = 11.5 Hz), (*m*-Ph), 129.8, d (J = 56.9 Hz), (ipso-Ph), 131.4, d (J = 31.2 Hz), (3-Py), 132.2, d (*J* = 2.5 Hz), (*p*-Ph), 133.0, s, (2-Thiol), 135.0, d (*J* = 13.7 Hz), (*o*- Ph), 136.3, s, (4-Thiol), 137.0, d (*J* = 10.4 Hz), (4-Py), 141.2, s, (1-Thiol), 151.7, d (*J* =

15.6 Hz), (6-Py), 155.2, d (J = 79.1 Hz), (ipso-Py). Anal. Calcd for $C_{46}H_{36}Au_2N_2P_2S_2$: C, 48.60; H, 3.19; N, 2.46; Found: C, 48.24; H 3.06; N, 2.28; MS(MALDI+/DIT): *m/e* = 1137.1 (15.5m%) $[M]^+$.

Synthesis of 6: This compound was prepared similarly to **1** using $ClAuPPh_3$ instead of $ClAuPPh_2Py$ and **L2** instead of **L1**. The product was obtained as a pale yellow solid (82.5 mg, 79% yield).

NMR (CD_2Cl_2 20°C): ^{31}P NMR (162 MHz) 37.13, s; ^1H NMR (400 MHz) 7.34 - 7.46, m, 6H (5-Py and 6- Thiol), 7.46 - 7.65, m, 20H (Ph, 3-Thiol and 2-Thiol), 7.68 - 7.78, m, 8H (Ph), 7.82, tdd (*J* = 7.7, 3.9, 1.8 Hz), 2H (4-Py), 7.85 - 7.92, m, 2H (3-Py), 8.77 - 8.84, m, 2H (6-Py); ^{13}C NMR (101 MHz) 125.6, d (*J* = 2.3 Hz), (5-Py), 126.7, s, (3-Thiol), 127.1, s, (2-Thiol), 129.5, d (*J* = 11.5 Hz), (*m*-Ph), 131.4, d (*J* = 30.9 Hz), (3-Py), 132.2, d (*J* = 2.5 Hz), (*p*-Ph), 133.0, s, (6-Thiol), 135.0, d (*J* = 13.8 Hz), (*o*-Ph), 135.9, s, (5-Thiol), 137.0, d (*J* = 10.4 Hz), (4-Py), 139.6, s, (4-thiol), 142.2, s, (1-Thiol), 151.7, d (*J* = 15.5 Hz), (6-Py).). Anal. Calcd for $C_{52}H_{40}Au_2N_2P_2S_2{\cdot}0.5CH_2Cl_2$: C, 50.23; H, 3.29; N, 2.23; Found: C, 50.10; H, 3.33; N, 2.05; MS (ES): m/z calcd for $C_{52}H_{40}P_2S_2N_2Au_2$ (M+) 1212.1, found 1213.2.

Synthesis of 7: This compound was prepared similarly to **1** using $ClAuPPh_3$ instead of $ClAuPPh_2Py$ and **L3** instead of **L1**. The product was obtained as a pale yellow solid (64.9 mg, 71 % yield).

NMR (CD_2Cl_2 20°C): ^{31}P NMR (162 MHz) 38.01, s; ^1H NMR (400 MHz) 7.02 - 7.07, m, 2H (3-Thiol), 7.37 - 7.43, m, 2H (5-Py), 7.43 – 7.5, m, 16H, (Ph and 2-Thiol), 7.64 – 7.75, m, 8H (Ph), 7.75 – 7.87, m, 4H (4-Py and 3-Py), 8.78, ddd (*J* = 3.9, 1.7, 0.8 Hz), 2H (6-Py); ^{13}C NMR (101 MHz) 126.1, d (*J* = 2.4 Hz), (5-Py), 129.9, d (*J* = 11.5 Hz), (*m*-Ph), 129.9, d (J = 57.1 Hz), (ipso-Ph), 131.3, s, (4-Thiol), 131.7, s, (3-Thiol), 131.8, d (*J* = 30.8 Hz), (3-Py), 132.6, d (*J* = 2.5 Hz), (*p*-Ph), 133.7, s, (2-Thiol), 135.4, d (*J* = 13.7 Hz), (*o*-Ph), 137.5, d (*J* = 10.3 Hz), (4-Py), 142.6, s, (1-Thiol), 152.1, d (*J* = 15.7 Hz), (6-Py), 155.5, d (*J* = 79.5 Hz), (ipso-Py). Anal. Calcd for $C_{48}H_{40}Au_2N_2P_2S_2$: C, 49.49; H, 3.46; N, 2.40 Found: C, 49.28; H 3.39; N, 2.24; MS(MALDI+/DIT): *m/e* = 1168.9 (18.73 %) $[M]^+$.

Synthesis of 8: This compound was prepared similarly to **1** using $ClAuPPh_3$ instead of $ClAuPPh_2Py$ and **L4** instead of **L1**. The product was obtained as a white solid (75.6 mg, 80 % yield).

NMR (CD_2Cl_2 20°C): ^{31}P NMR (162 MHz) 35.97, s wide; NMR ($CDCl_3$ 20°C): ^1H NMR (400 MHz) 4.24, s, 4H (1- Thiol), 7.25 – 7.29, m, 2H (4-Py), 7.29 – 7.33, m, 4H (4-Thiol), 7.33 – 7.47, m, 12H (Ph), 7.49 – 7.64, m, 14H (Ph, C-Py and 3-Thiol), 7.70, t (*J* = 7.5 Hz), 2H (4-Py), 8.71, ddd (*J* = 3.9, 1.7, 0.8 Hz), 2H (6-Py); ^{13}C NMR (101 MHz) 32.6, s, (1-Thiol), 125.0, d (*J* = 2.2 Hz), (5-Py), 127.0, s, (4-Thiol), 128.9, s, (3-Thiol), 129.0, d (*J* = 2.4 Hz), (*m*-Ph), 131.4, d (*J* = 32.3), (3-Py), 131.5, d (*J* = 2.3 Hz), (*p*-Ph), 134.6, d (*J* = 14.1 Hz), (*o*-Ph), 136.43, d (*J* = 10.6 Hz), (4-Py), 138.6, s, (5-Thiol), 146.7, s, (2-Thiol), 151.2, d (*J* = 14.4 Hz), (6-Py). Anal. Calcd for $C_{46}H_{36}Au_2N_2P_2S_3$: C, 47.27; H, 3.10; N, 2.40, Found: C, 46.94; H 3.29; N, 2.15; MS(MALDI+/DIT): *m/e* = 1164.9 (18.80 %) $[M]^+$.

Crystallography

The crystals were mounted in inert oil on glass fibers and transferred to the cold gas stream of an Xcalibur Oxford Diffraction (**2**, **4**, **6**) or a Bruker Smart 1000 CCD (**5**) diffractometer equipped with a low-temperature attachment. Data were collected using monochromated Mo Kα radiation (λ= 0.71073 Å). Scan type: ω. Absorption correction based on multiple scans was applied using spherical harmonics implemented in SCALE3 ABSPACK[18] scaling algorithm (**2**, **4**, **6**) or with a program SADABS (**5**). The structures were solved by direct methods and refined on F^2 using the program SHELXL-97.[19] All non-hydrogen atoms were refined anisotropically. In all cases, hydrogen atoms were included in calculated positions and refined using a riding model. Refinements were carried out by full-matrix least-squares on F^2 for all data. Additional details of the data collection and refinement are given in Table 3. Further details of the crystal structure investigation are available free of charge from The Cambridge Crystallographic Data Center via www.ccdc.cam.ac.uk/data_request/cif on quoting the depository numbers CCDC 976386 (**2**), CCDC 976387 (**4**), CCDC 976388 (**5**) and CCDC 976389 (**6**).

DFT calculations

Quantum-chemical calculations based on the Density Functional Theory (DFT) were carried out on compounds **4** and **5'** by adopting the mPW1PW[19] functional and using the commercial suite of programs Gaussian09.[20] Schäfer, Horn, and Ahlrichs double-ζ plus polarization all-electron basis sets (BSs)[21] were used for all atomic species but gold, for which SBKJC BSs[22] with relativistic effective core potentials (RECP) were adopted. The geometry optimizations (with tight cut-off values on forces and step size) were performed without introducing any structural simplification or symmetry restrain. In all cases, a pruned (99,590) grid was adopted in order to avoid imaginary frequencies. NBO populations[23] and Wiberg bond indices[24] were calculated at the optimized geometries. Time-dependent (TD) DFT calculations were carried out in order to understand their absorption/emission spectroscopic features. The programs GaussView[25] and Molden 5.0[26] were used to investigate the natural charge distributions and MOs' shapes and to generate the simulated absorption spectra based on TD-DFT calculations.

5

Table 3. X-ray crystallographic data of complexes **2, 4, 5** and **6.**

Compound	2	4	5	6
Formula	$C_5H_{42}Au_2P_2S_2 \cdot 2(CH_2Cl_2)$	$C_{50}H_{42}Au_2P_2S_2$	$C_{46}H_{36}Au_2N_2P_2S_2$	$C_{52}H_{40}Au_2N_2P_2S_2$
M_r	1380.72	1162.83	1136.76	1212.85
Crystal size (mm)	0.070 × 0.06 × 0.05	0.24 × 0.18 ×	0.24 × 0.20 ×	0.07 × 0.06 ×
Crystal system	Monoclinic	Monoclinic	Monoclinic	Triclinic
Space group	C2/c	P2(1)/n	C2/c	P-1
Cell constants:				
***a* (Å)**	23.2023(4)	14.4157(2)	14.480(3)	8.0066(16)
***b* (Å)**	13.8267(2)	9.02110(10)	15.850(3)	10.946(2)
***c* (Å)**	18.1353(3)	16.5956(2)	16.890(3)	13.085(3)
α (°)	90	90	90	83.58(3)
β (°)	104.409(2)	105.8050(10)	97.86(3)	73.91(3)
γ (°)	90	90	90	80.08(03)
***V* (Å^3)**	5635.0(16)	2076.59(4)	3840.0(13)	1082.9(4)
Z	4	2	4	1
D_x **(Mg m^{-3})**	1.628	1.860	1.966	1.860
μ(mm^{-1})	5.456	7.270	7.862	6.976
***F*(000)**	2680	1124	2184	586
***T* (K)**	100(2)	100(2)	100(2)	100(2)
$2\theta_{max}$	55	55	55	55
No. of refl.:				
measured	27864	20406	24212	6385
independent	5209	3838	3558	4002
Transmissions	0.7686 – 0.6971	0.4758 -	0.3319 – 0.2541	0.7218 – 0.6409
R_{int}	0.0323	0.0209	0.0567	0.0628
Parameters	334	253	245	271
Restraints	56	0	0	0
Goodness of fit on F^2	1.068	1.059	1.023	1.026
***wR*(F^2, all Refl.)**	0.0746	0.0333	0.0998	0.0790
***R*($I > 2\sigma(I)$)**	0.0287	0.0133	0.0383	0.0489
max. Δρ (e Å^{-3})	2.255	0.430	2.600	1.209

Acknowlegdgements

The authors gratefully acknowledge the Ministerio de Economía y Competitividad-FEDER (CTQ2010-20500-C01-C02) and DGA-FSE (E77) for financial support. VL and MA also thank Università degli Studi di Cagliari for financial support.

Supplementary info:

† Electronic Supplementary Information (ESI) available: structural features in the packing of complexes 2, 4, 6 (Figs. S1-S4); DRUV spectra of L1-L4 (Fig. S5); DRUV spectra of complexes 2-**4**, **6**-**8** (Fig. S6); emission spectra of complexes **2**, **4**, **5**, **7** (Fig. S7); simulated absorption spectrum of **4** in the gas phase (Fig. S8); isosurface drawings of selected Kohn-Sham MOs calculated for **4** (Fig. S9).

Notes and references

[a] *Departamento de Química Inorgánica, Instituto de Síntesis Química y Catálisis Homogénea (ISQCH), CSIC- Universidad de Zaragoza, 50009 Zaragoza, Spain. Fax: +34 976761187 Tel: +34 976762291; E-mail: gimeno@unizar.es*

[b] *Dipartimento di Scienze Chimiche e Geologiche, Università degli Studi di Cagliari, S.S. 554 Bivio per Sestu, 09042-Monserrato(CA), Italy*

1 (a) J. C. Lima, L. Rodríguez, *Chem. Soc. Rev.*, **2011**,40, 5442–5456, (b) M. O. Awaleh, F. Baril-Robert, C. Reber, A. Badia, F. Brise, *Inorg. Chem.*, **2008**, 47, 2964. (c) E. J. Fernández, A. Laguna, J. M. López-de Luzuriaga, *Dalton Trans.*, **2007**, 1969.

2 (a) X. He, V. W.-W.Yam, *Coord. Chem. Rev.*, **2011**, 255, 2111; (b) X. He, V. W.-W.Yam, *Inorg. Chem.*, **2010**, 49, 2273; (c) X. He, F. Herranz, E. C.-C. Cheng, R. Vilar, V. W.-W Yam, *Chem.-Eur. J.*, **2010**, 16, 9123.

3 K. P. Bhabak, B. J. Bhuyan, G. Mugesh, *Dalton Trans.*, **2011**,40, 2099, I. Ott, *Coord. Chem. Rev.*, **2009**,253, 1670.

[4] (a) B.-C. Tzeng, H.-T. Yeh, Y.-C. Huang, H.-Y. Chao, G.-H. Lee, S.-M. Peng, *Inorg. Chem.* **2003**, *42*, 6008-6014, (b) H. Ehlich, A. Schier, H. Schmidbaur, *Inorg. Chem.* **2002**, *41*, 3721-3727, (c) M. C. Gimeno, P. G. Jones, A. Laguna, M. Laguna, R. Terroba, *Inorg. Chem.*, **1994**, 33, 3932-3938

[5] (a) V. Wing-Wah Yam, C.-L. Chan, C.-K. Li, K. Man-Chung Wong, *Coord. Chem. Rev.*, **2001**, 216–217, 173; (b) E. R. T. Tiekink, J.-G. Kang, *Coord. Chem. Rev.*, **2009**, 25-3, 1627.

[6] I. O. Koshevoy, E. S. Smirnova,M. Haukka, A. Laguna, J. C. Chueca,T. A. Pakkanen, S. P. Tunik, I. Ospino, O. Crespo, *Dalton Trans.*, **2011**, 40, 7412.

[7] (a) M. Bardají, M. J. Calhorda, P. J. Costa, P. G. Jones, A. Laguna, M. R. Pérez, M. D. Villacampa, *Inorg. Chem.*, **2006**, 45, 1059. (b) W. J. Hunks, M. C. Jennings, R. J. Puddephatt, *Inorg. Chim. Acta*,, **2006**, 359, 3605, (c) J. M. Forward, D. Bohmann, Jr. J. P. Flacker, R. J. Staples, *Inorg. Chem*., **1995**, 34, 6330.

[8] (a) E. J. Fernández, A. Laguna, J. M. López-de-Lurriaga, M. Monge, M. Montiel, M. E. Olmos, R. C. Puelles, E. Sánchez-Forcada, *Eur. J. Inorg. Chem.*, **2007**, 4001.(b) J. D. E. T. Wilton-Ely, A. Schier, N. W. Mitzel, H. Schmidbaur, *J. Chem. Soc*., *Dalton Trans*., **2001**, 1058. (c) R. Narayanaswamy, M. A. Young, E. Parkhurst, M. Ouellette, M. E. Kerr, D. M. Ho, R. C. Elder, A. E. Bruce, M. R. M. Bruce, *Inorg Chem.*, **1993**, 32, 2506.

[9] C. Janiak, *J. Chem. Soc., Dalton Trans.*, **2000**, 3885.

[10] (a) H. Schmidbaur, *Chem. Soc. Rev.* **1995**, 391-400, (b) L. Hao, R. J. Lachicotte, H. J. Gysling, R. Eisenberg, *Inorg Chem.*, **1999**, 38, 4616.

[11] S. Y. Ho, E. C.-C. Cheng, E. R. T. Tieknik, V. W.-W. Yam, *Inorg. Chem.*, **2006**, 45, 8165.

[12] B.-C. Tzeng, C.-K. Chan,K.-K. Cheung, C.-M. Che, S.-M. Peng, *Chem. Commun.*, **1997**, 135.

[13] (a) M. J. Calhorda, C. Ceamanos, O. Crespo, M. C. Gimeno, A. Laguna, C. Larraz, P. D. Vaz, M. D. Villacampa, *Inorg. Chem.*, **2010**, 49, 8255; (b) R. F. Ziolo, S. Lipton, Z. Dori, *Chem. Commun.*, **1970**, 1124.

[14] (a) J. Cámara, O. Crespo, M. C. Gimeno, I. O. Koshevoy, A. Laguna, I. Ospino, E. S. Smirnova, S. P. Tunik, *Dalton Trans.*, **2012**, 41, 13891.

[15] J. P. Fackler Jr, Z. Assefa, J. M. Forward, R. J. S Taples, *Metal based drugs*, **1994**, 1, 459

[16] (a) C. King, M. N. I. Khan, R. J. Staples, J. P. Fackler Jr, *Inorg. Chem.*, **1992,** 31, 3236-3238; (b) L. Hao, M. A. Mansour, R. J. Lachotte, H. J. Glysling, R. Eisenberg, *Inorg. Chem.*, **2000,** 39, 5520.

[17] (a) R. Uson, A. Laguna, *Organomet. Synth.*, **1985**, 3, 325. (b) L. Malatesta, L. Naldini, G. Simonetta, F. Cariati, *Coord. Chem. Rev.*, **1966**, 1, 255.

[18] CrysAlisPro, Agilent Technologies, Version 1.171.35.11. Multi-scans absorption correction with SCALE3 ABSPACK scaling algorithm.

[19] G. M. Sheldrick, SHELXL-97, Program for Crystal Structure Refinement, University of Göttingen, Göttingen, Germany, 1997.

[19] C. Adamo, V. Barone, *J. Chem. Phys*. **1998**, *104*, 664.

[20] Gaussian 09, Revision A02, M. J. Frisch, G. W. Trucks, H. B. Schlegel, G. E. Scuseria, M. A. Robb, J. R. Cheeseman, G. Scalmani, V. Barone, B. Mennucci, G. A. Petersson, H. Nakatsuji, M. Caricato, X. Li, H. P. Hratchian, A. F. Izmaylov, J. Bloino, G. Zheng, J. L. Sonnenberg, M. Hada, M. Ehara, K. Toyota, R. Fukuda, J. Hasegawa, M. Ishida, T. Nakajima, Y. Honda, O. Kitao, H. Nakai, T. Vreven, J. A. Montgomery, Jr., J. E. Peralta, F. Ogliaro, M. Bearpark, J. J. Heyd, E. Brothers, K. N. Kudin, V. N. Staroverov, R. Kobayashi, J. Normand, K. Raghavachari, A. Rendell, J. C. Burant, S. S. Iyengar, J. Tomasi, M. Cossi, N. Rega, J. M. Millam, M. Klene, J. E. Knox, J. B. Cross, V. Bakken, C. Adamo, J. Jaramillo, R. Gomperts, R. E. Stratmann, O. Yazyev, A. J. Austin, R. Cammi, C. Pomelli, J. W. Ochterski, R. L. Martin, K. Morokuma, V. G. Zakrzewski, G. A. Voth, P. Salvador, J. J. Dannenberg, S. Dapprich, A. D. Daniels, Ö. Farkas, J. B. Foresman, J. V. Ortiz, J. Cioslowski, and D. J. Fox, Gaussian, Inc., Wallingford CT, 2009.

[21] A. Schäfer, H. Horn, R. Ahlrichs, *J. Chem. Phys.* **1992**, *97*, 2571.

[22] W. J. Stevens, M. Krauss, H. Basch, P. G. Jasien, *Can. J. Chem*. **1992**, *70*, 612.

[22] a) A. E. Reed, F. Weinhold, *J. Chem. Phys*. **1983**, *78*, 4066; b) A. E. Reed, R. B. Weinstock, F. Weinhold, *J. Chem. Phys*. **1985**, *83*, 735; c) A. E. Reed, L. A. Curtiss, F. Weinhold, *Chem. Rev.* **1988**, *88*, 899.

[24] K. Wiberg, *Tetrahedron* **1968**, *24*, 1083.

[25] GaussView, Version 5, R. Dennington, T. Keith, J. Millam, Semichem Inc., Shawnee Mission KS, 2009.

[26] G. Schaftenaar, J. H. Noordik, *J. Comput.–Aided Mol. Design* **2000**, *14*, 123.